

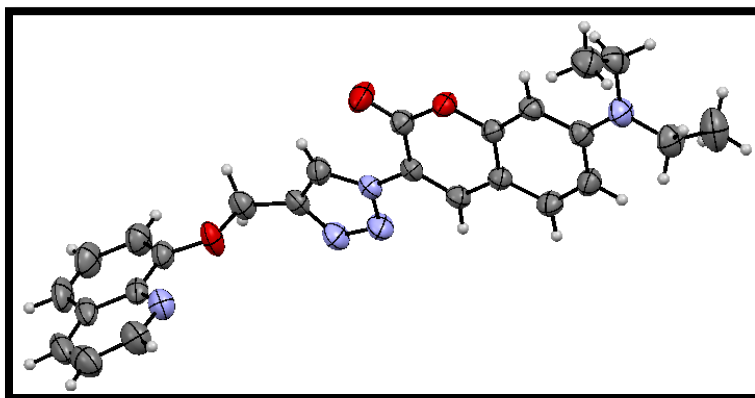
Supporting Information

Unusual absence of FRET in triazole bridged coumarin-hydroxyquinoline, an effective sensor for Hg²⁺ detection

Surajit Mondal^a, Niladri Patra^{*a}, Hari Pada Nayek^a, Sumit K. Hira^b, Soumit Chatterjee^{*a} and Swapan Dey^{*a}

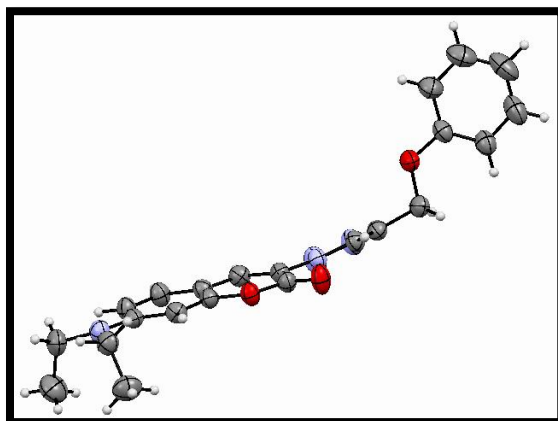
Sl. No.	Table of content	Page No.
1	Crystal structures and Crystallographic data for R1 , R2 and R3	2-4
2	¹ H NMR, ¹³ C NMR, Mass and FT-IR spectra of compound 2, compound 3, compound 4, R1 , R2 and R3	5-15
3	Mass and FT-IR spectra of complex (R1+Hg ²⁺)	15
4	Table T1: Fluorescence decay parameters of coumarin amine (C)-quinoline (Q) mixtures and R1 at λ _{em} = 485 nm and 420 nm.	16
5	Table T2: Excited state decay parameters of R1 with Hg ²⁺	16
6	Table T3: Binding energy from DFT calculation	16
7	Fig. S1: Titration spectra; in UV-vis (a) R2:Hg ²⁺ , (c) R3+ Hg ²⁺ , and in fluorescence (b) R2:Hg ²⁺ , (d) R3:Hg ²⁺	17
8	Fig. S2: Sensing behavior of R1 towards Hg ²⁺ under long UV	17
9	Fig. S3: S-V plots from steady state fluorescence emission intensity measurements.	18
10	Fig. S4: Lifetime measurement with other metal ion.	18
11	Fig. S5: Fluorescence decay traces of R1 and quinoline-coumarin mixture (2:1) at λ _{em} = 485 nm and 420 nm.	19
12	Fig. S6: Binding constant calculation graph of R1 with Hg ²⁺ using Fluorescence titration by using linear regression analysis	20
13	Fig. S7: LOD calculation curve of R1 with Hg ²⁺	20
14	Reversibility test of receptor	21
15	Fig. S10 Job's Plot	22
16	Fig. S12: Energy diagram for d-PET mechanism.	23
17	Table T4: Comparative table of triazole based sensor for Hg ²⁺ from reported literature	24
18	Synthesis procedure of coumarin azide	24

Crystallographic data for R1



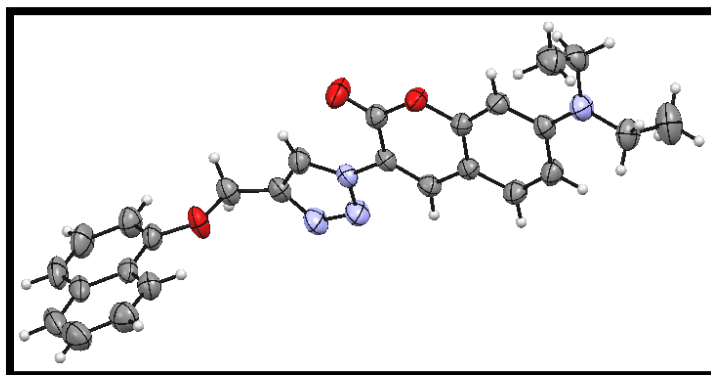
Identification code	R1
CCDC number	1944133
Empirical formula	C ₂₅ H ₂₃ N ₅ O ₃
Formula weight	441.48
Temperature/K	293(2)
Crystal system	triclinic
Space group	P-1
a/Å	9.6779(8)
b/Å	10.4548(10)
c/Å	12.1262(10)
α/°	112.874(9)
β/°	91.882(7)
γ/°	103.594(7)
Volume/Å ³	1088.16(18)
Z	2
ρ _{calc} /cm ³	1.347
μ/mm ⁻¹	0.091
F(000)	464.0
Crystal size/mm ³	0.15 × 0.13 × 0.11
Radiation	MoKα (λ = 0.71073)
2θ range for data collection/°	4.372 to 53.998
Index ranges	-12 ≤ h ≤ 12, -13 ≤ k ≤ 13, -15 ≤ l ≤ 15
Reflections collected	9010
Independent reflections	4680 [R _{int} = 0.0204, R _{sigma} = 0.0451]
Data/restraints/parameters	4680/0/298
Goodness-of-fit on F ²	0.994
Final R indexes [I ≥ 2σ (I)]	R ₁ = 0.0513, wR ₂ = 0.1163
Final R indexes [all data]	R ₁ = 0.0977, wR ₂ = 0.1334
Largest diff. peak/hole / e Å ⁻³	0.15/-0.21

Crystallographic data for R2



Identification code	R2
CCDC number	1904920
Empirical formula	C ₂₂ H ₂₂ N ₄ O ₃
Formula weight	390.43
Temperature/K	293(2)
Crystal system	monoclinic
Space group	P2 ₁ /c
a/Å	9.5210(11)
b/Å	19.764(2)
c/Å	10.8022(12)
α/°	90
β/°	103.759(12)
γ/°	90
Volume/Å ³	1974.4(4)
Z	4
ρ _{calc} /cm ³	1.314
μ/mm ⁻¹	0.090
F(000)	824.0
Crystal size/mm ³	0.16 × 0.02 × 0.01
Radiation	MoKα (λ = 0.71073)
2θ range for data collection/°	4.122 to 58.738
Index ranges	-13 ≤ h ≤ 11, -25 ≤ k ≤ 25, -11 ≤ l ≤ 14
Reflections collected	9990
Independent reflections	4606 [R _{int} = 0.0271, R _{sigma} = 0.0468]
Data/restraints/parameters	4606/0/264
Goodness-of-fit on F ²	1.180
Final R indexes [I ≥ 2σ (I)]	R ₁ = 0.0546, wR ₂ = 0.1366
Final R indexes [all data]	R ₁ = 0.0998, wR ₂ = 0.1536
Largest diff. peak/hole / e Å ⁻³	0.13/-0.20

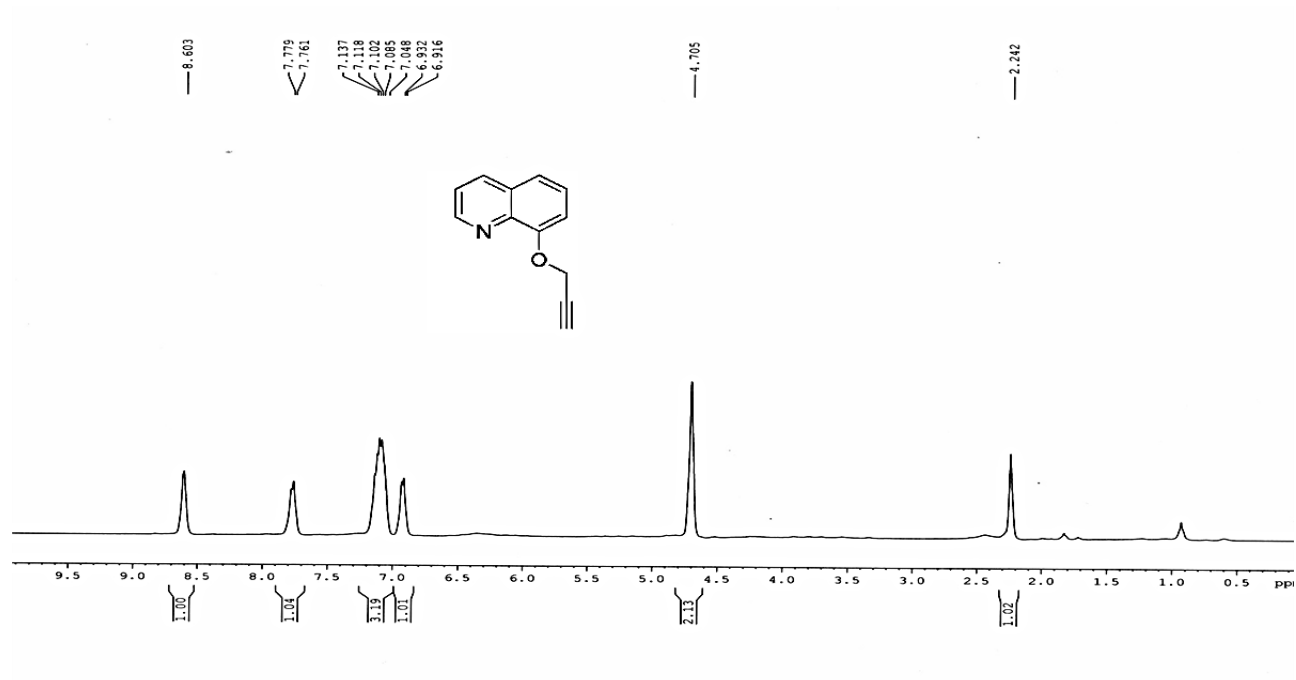
Crystallographic data for R3



Identification code	R3
CCDC number	1904921
Empirical formula	C ₂₆ H ₂₄ N ₄ O ₃
Formula weight	440.49
Temperature/K	293(2)
Crystal system	triclinic
Space group	P-1
a/Å	9.5658(8)
b/Å	10.6286(15)
c/Å	12.2495(15)
α/°	113.080(12)
β/°	91.151(8)
γ/°	103.715(9)
Volume/Å ³	1104.1(2)
Z	2
ρ _{calc} /cm ³	1.325
μ/mm ⁻¹	0.089
F(000)	464.0
Crystal size/mm ³	0.15 × 0.02 × 0.01
Radiation	MoKα (λ = 0.71073)
2θ range for data collection/°	4.322 to 58.704
Index ranges	-10 ≤ h ≤ 12, -14 ≤ k ≤ 9, -16 ≤ l ≤ 15
Reflections collected	9589
Independent reflections	5107 [R _{int} = 0.0250, R _{sigma} = 0.0556]
Data/restraints/parameters	5107/0/300
Goodness-of-fit on F ²	1.027
Final R indexes [I ≥ 2σ (I)]	R ₁ = 0.0536, wR ₂ = 0.1144
Final R indexes [all data]	R ₁ = 0.1137, wR ₂ = 0.1387
Largest diff. peak/hole / e Å ⁻³	0.13/-0.21

Characteristic experimental data

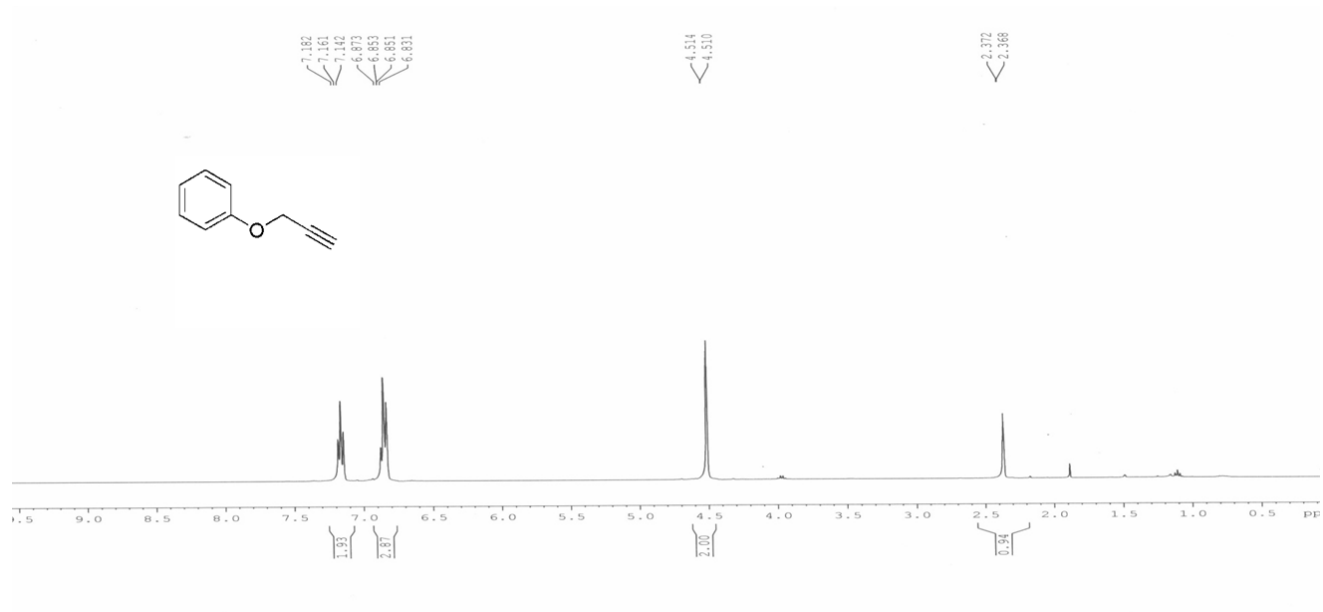
^1H NMR (400 MHz, CDCl_3) of Compound 2:



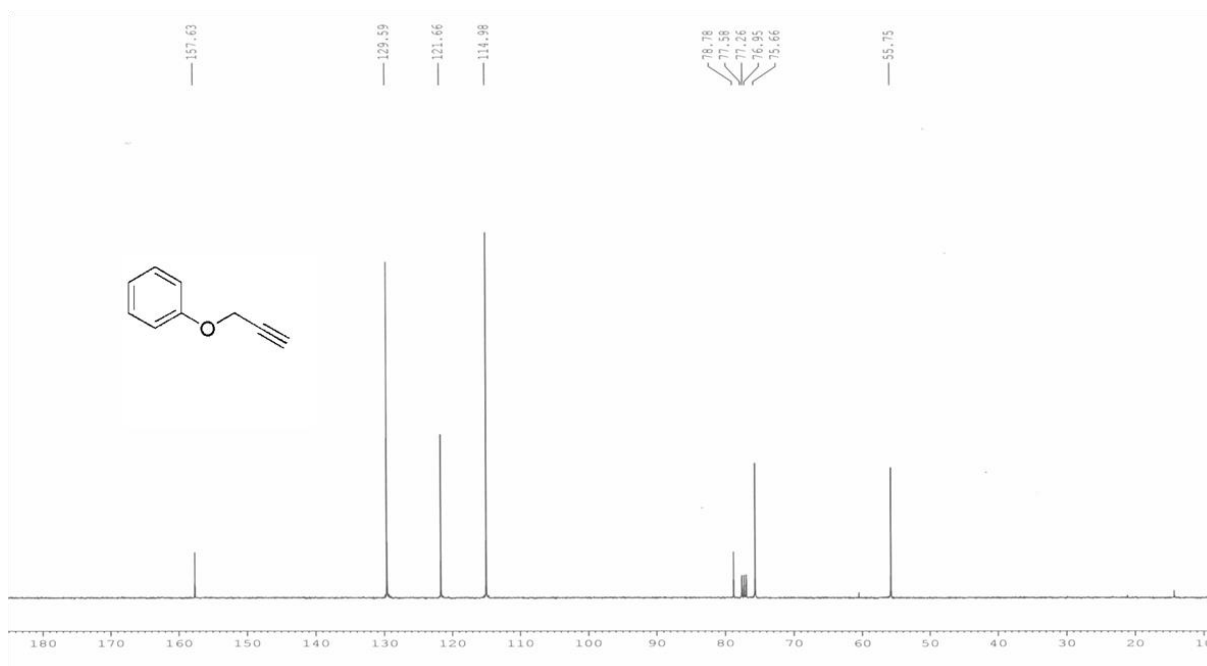
^{13}C NMR (100 MHz, CDCl_3) of Compound 2:



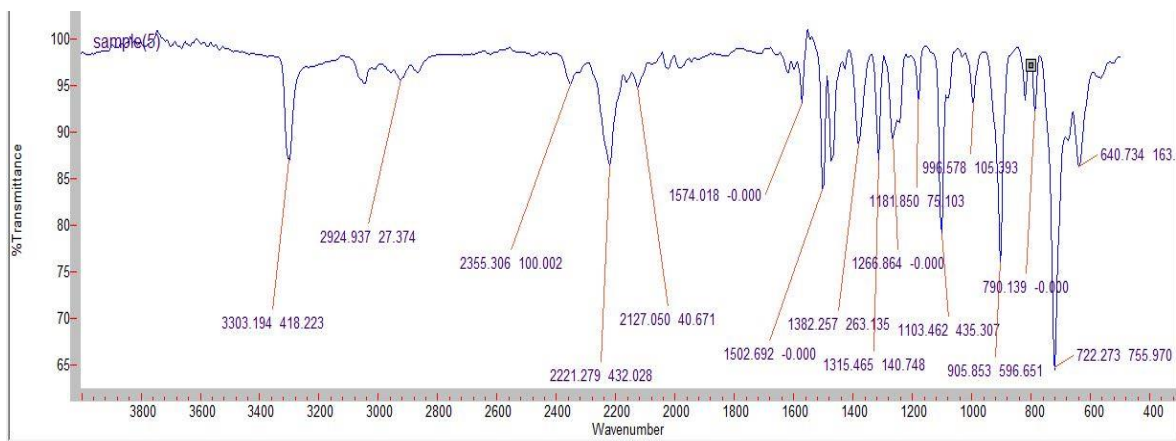
¹H NMR (400 MHz, CDCl₃) of compound 3:



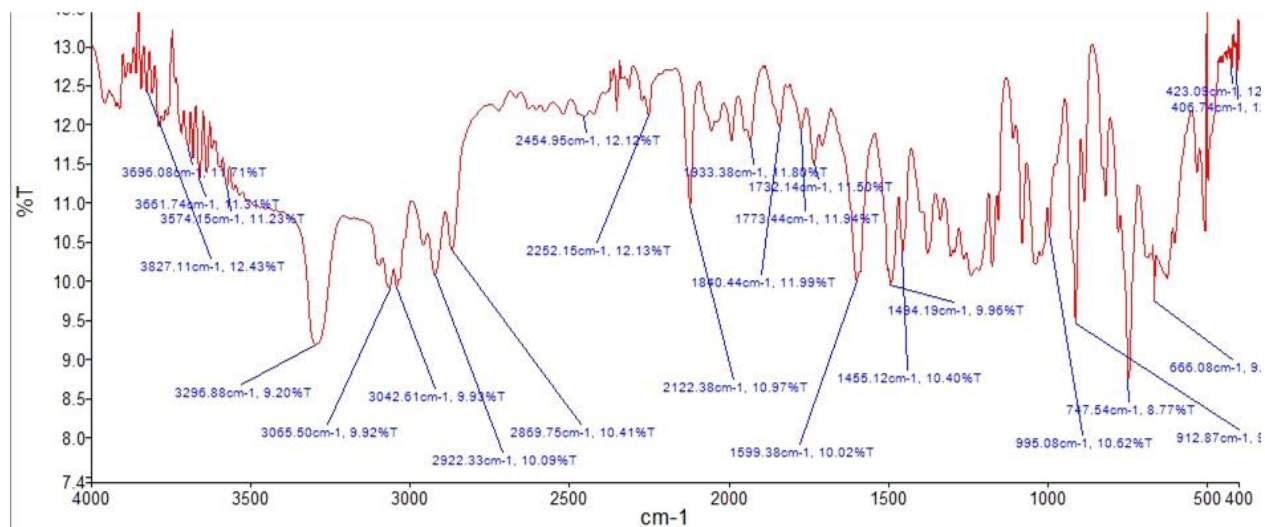
¹³C NMR (100 MHz, CDCl₃) of compound 3:



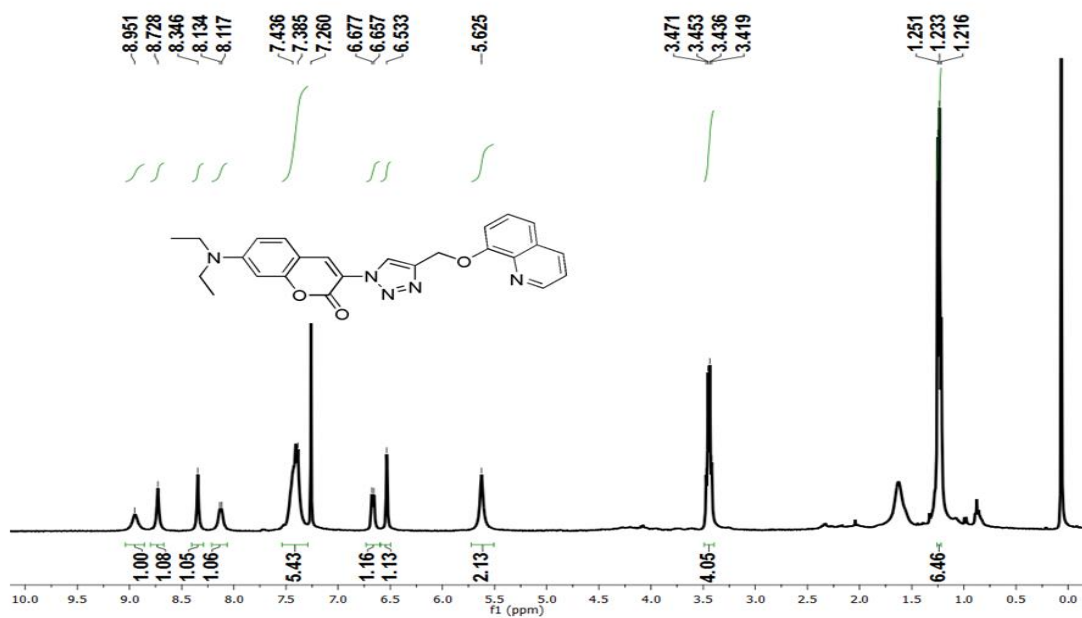
FT-IR spectra of compound 2



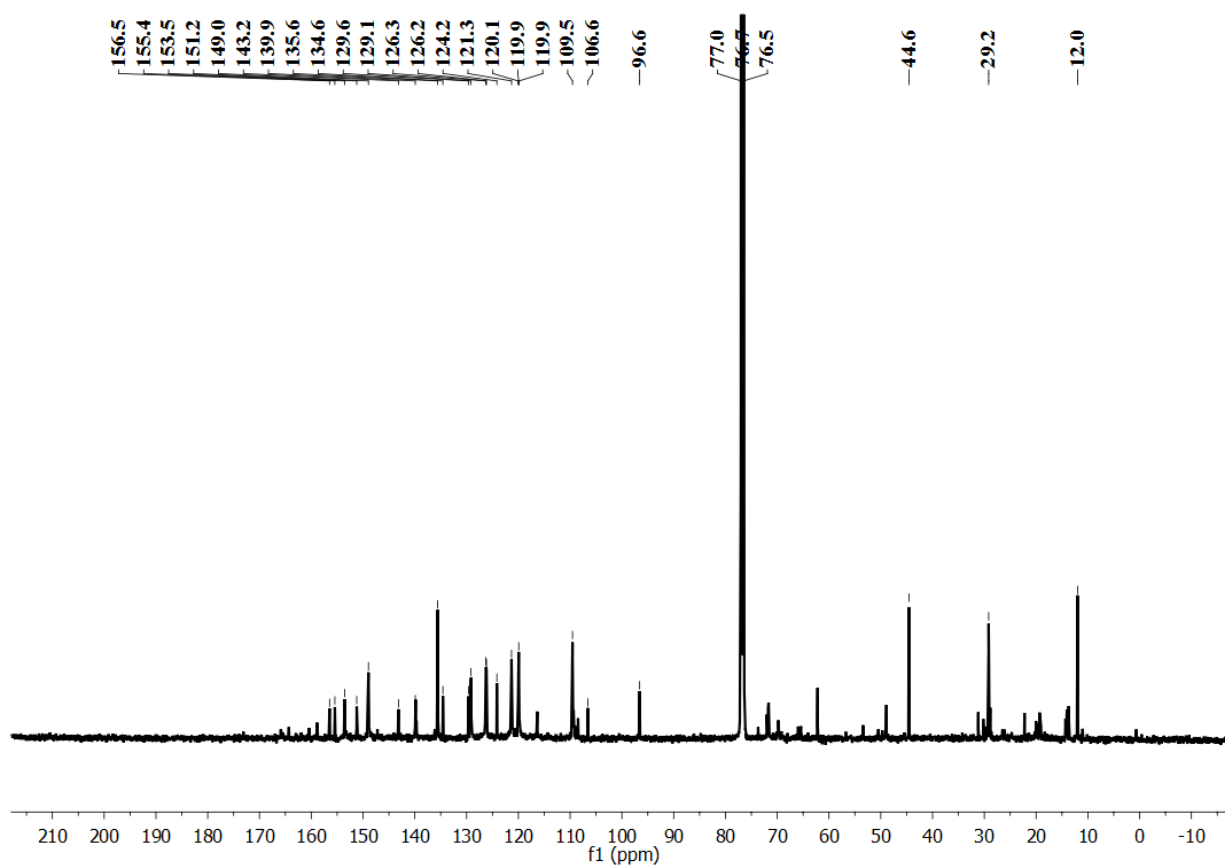
FT-IR spectra of compound 3:



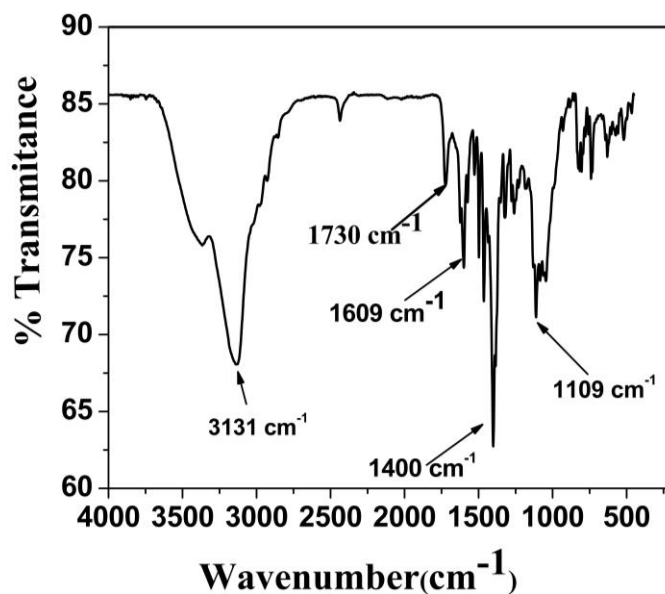
¹H NMR of R1 (400 MHz, CDCl₃):



¹³C NMR of R1 (125 MHz, CDCl₃):

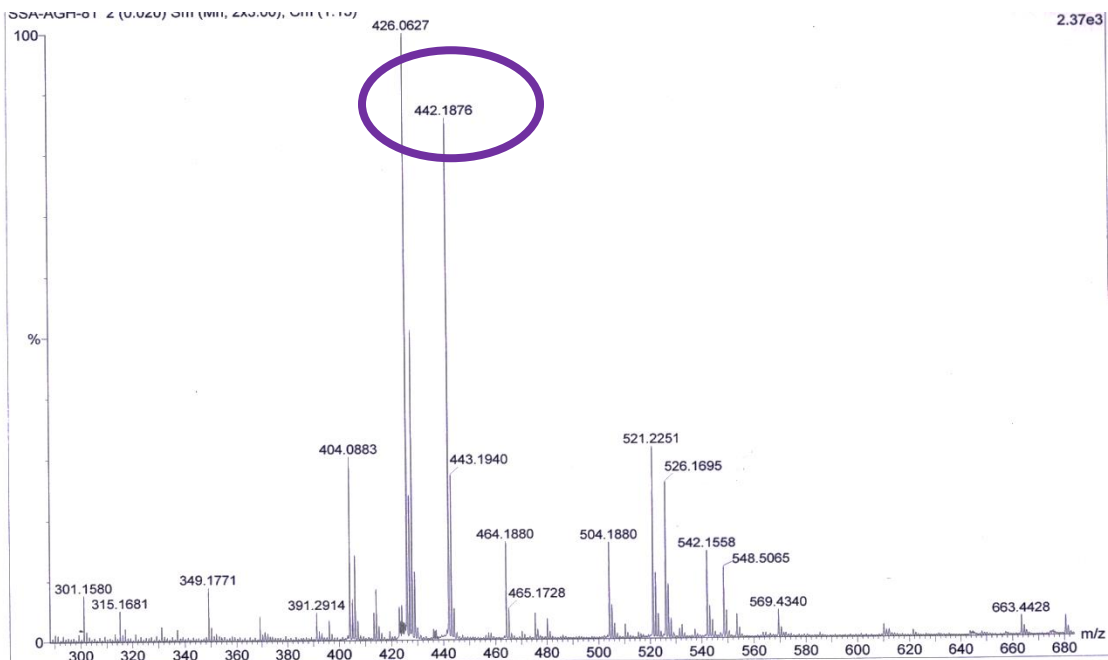


FT-IR spectra of R1:

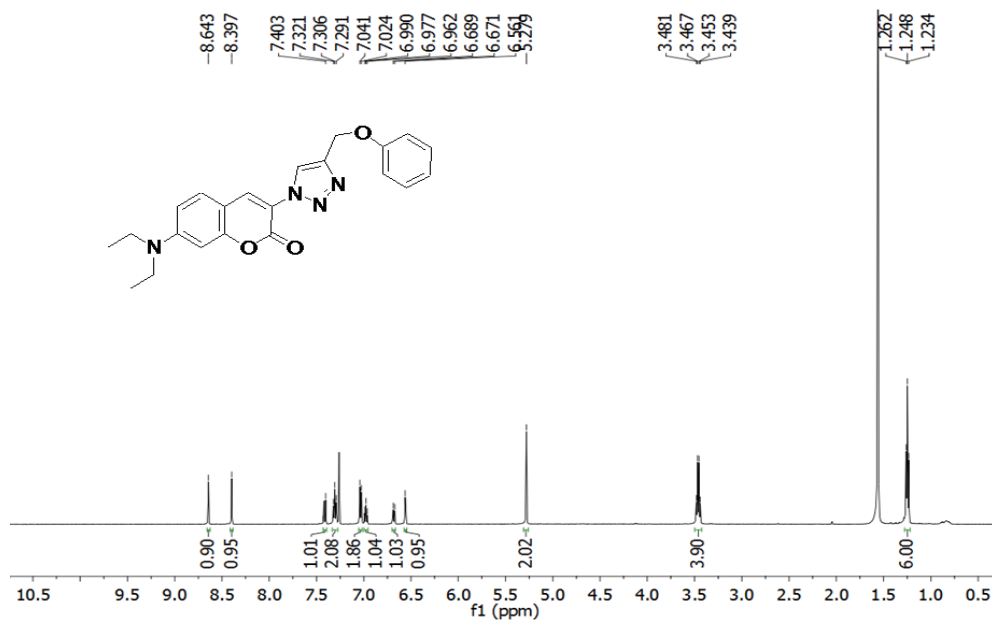


HRMS Spectra (R1):

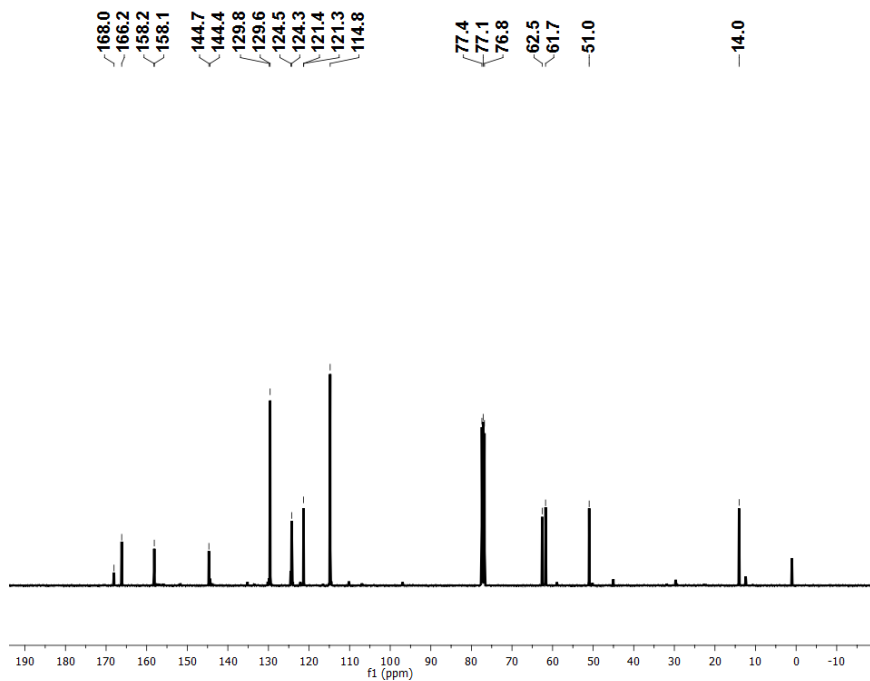
Calculated: 441.1801, Found: 442.1874 [M+H]⁺



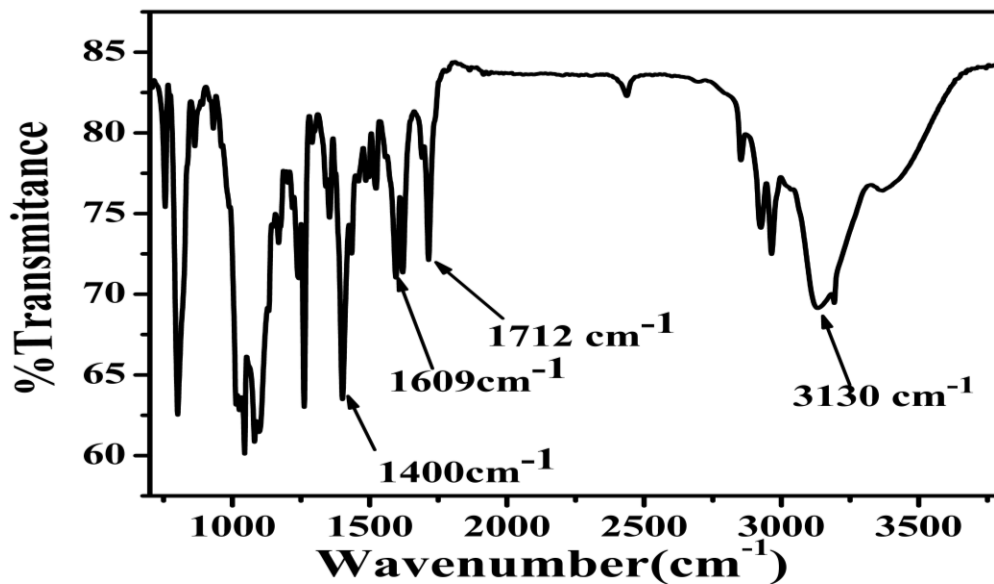
¹H NMR of R2 (500 MHz, CDCl₃):



¹³C NMR of R2 (100 MHz, CDCl₃)

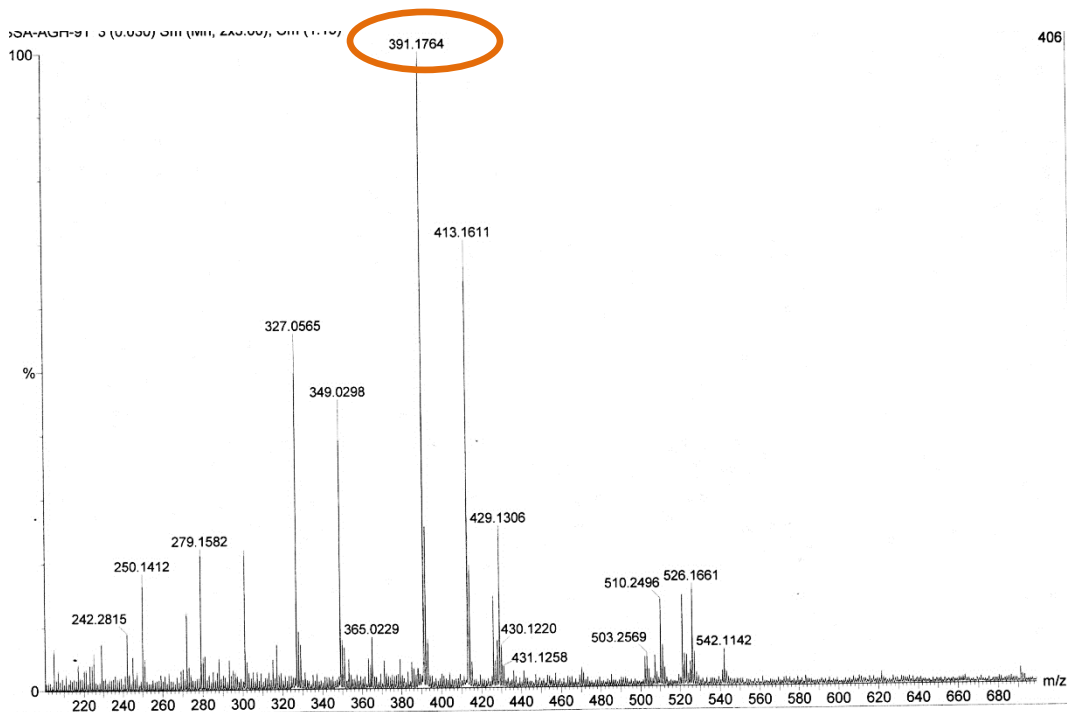


FT-IR Spectra of R2

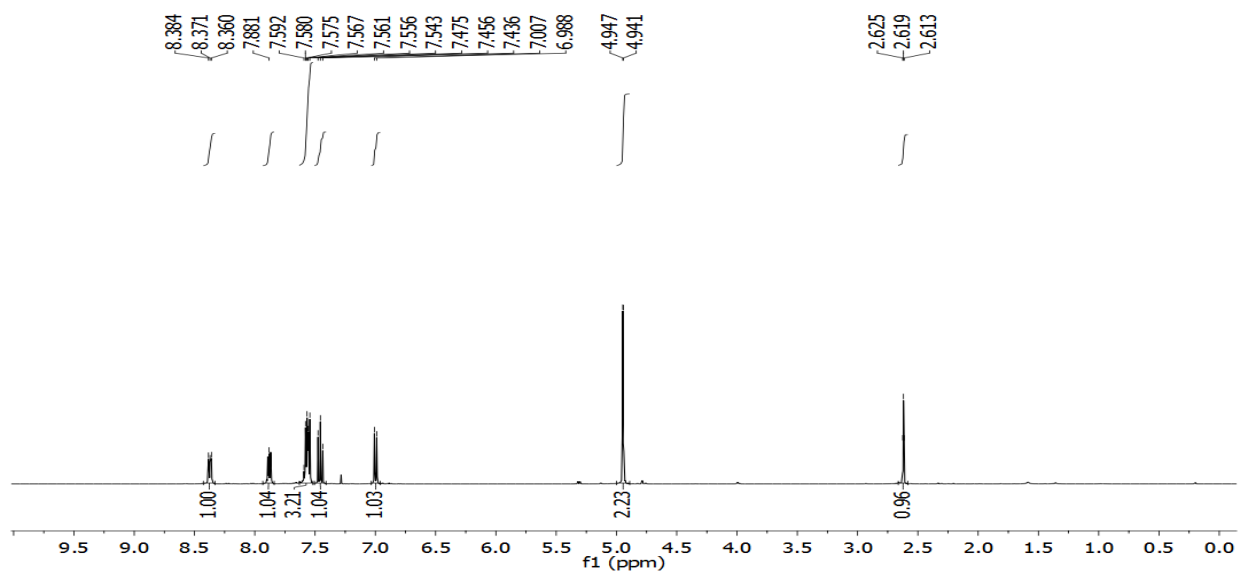


HRMS Spectra (R2):

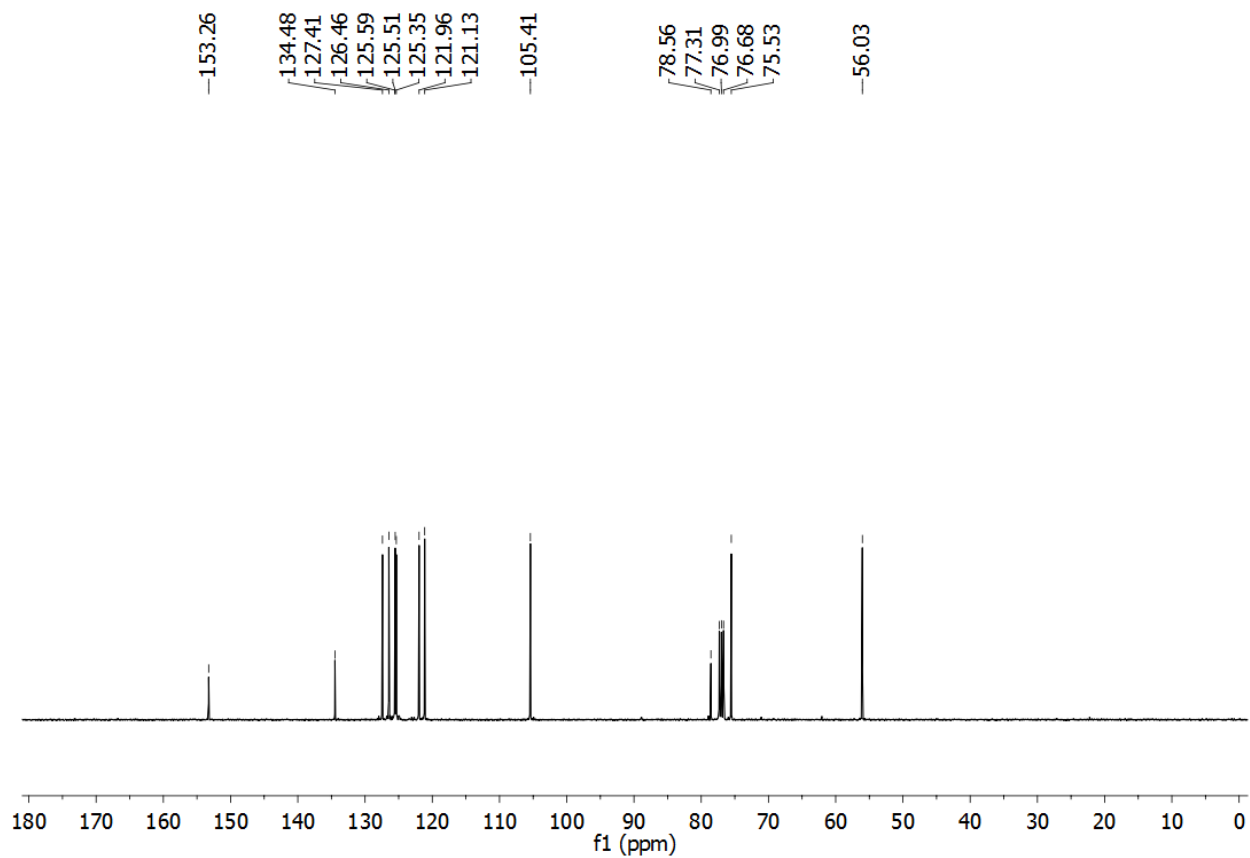
Calculated: 390.4351, Mass: 391.1765 [M+H]⁺



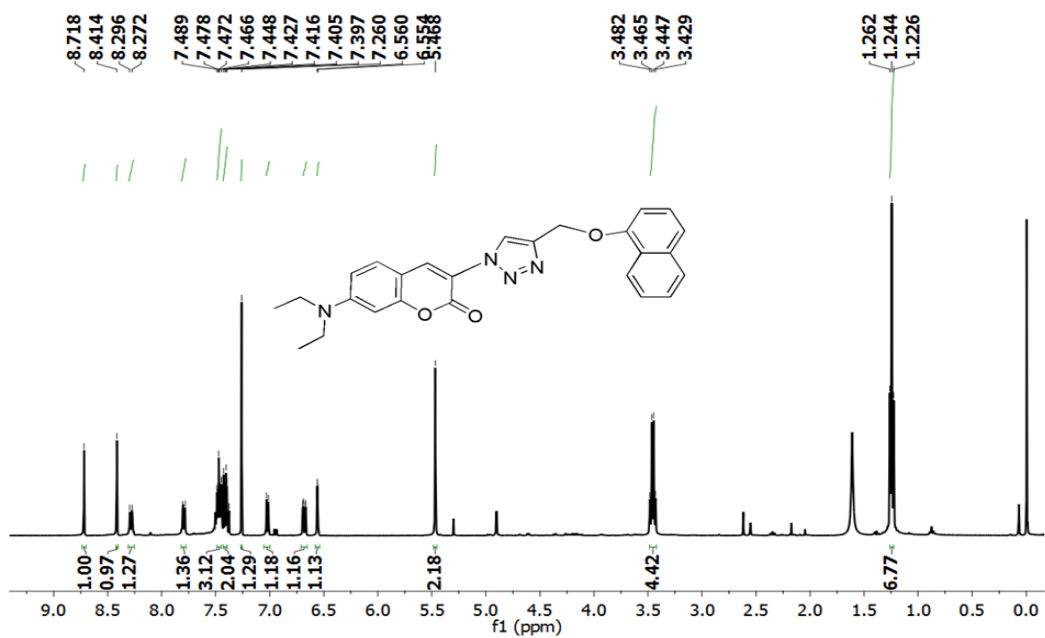
^1H NMR (400 MHz, CDCl_3) of Compound 4:



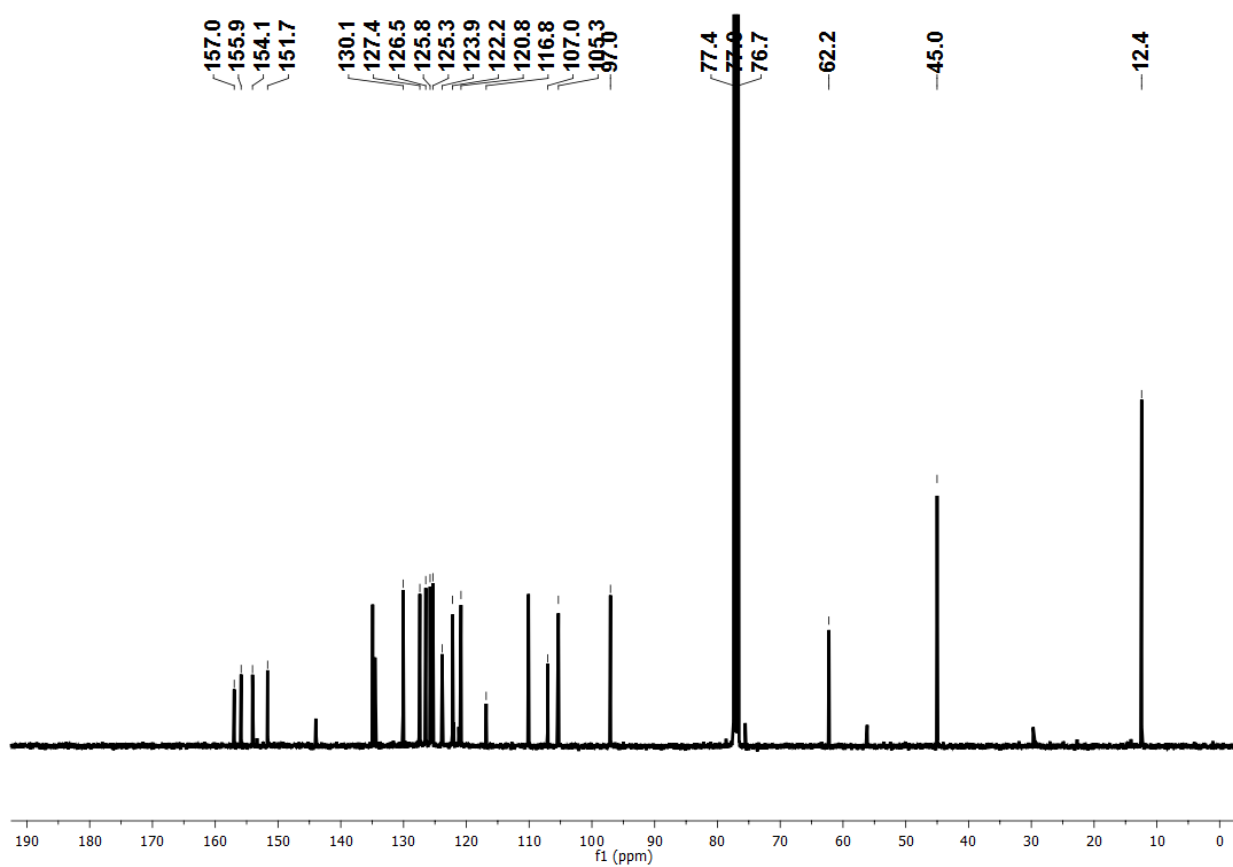
^{13}C NMR (100 MHz, CDCl_3) of Compound 4:



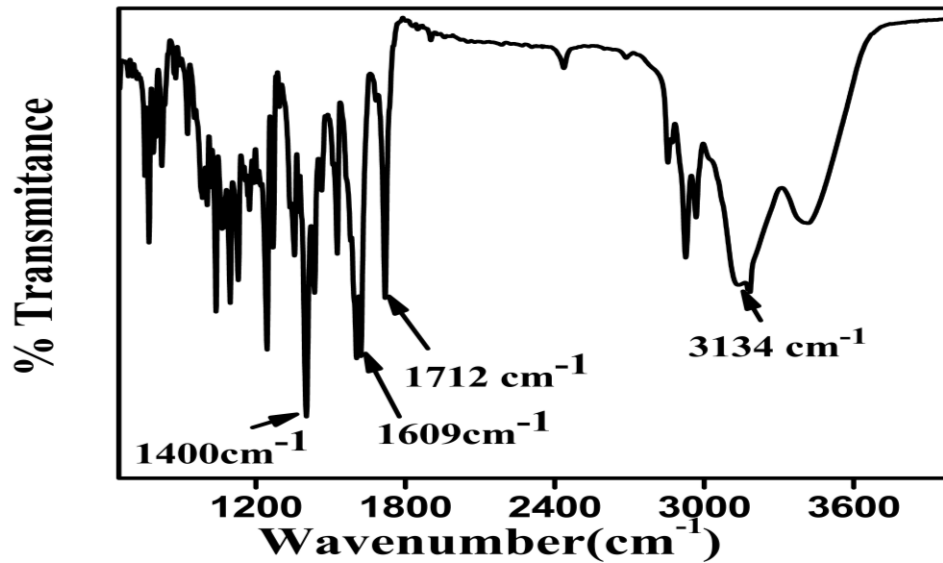
¹H NMR of R3 (400 MHz, CDCl₃):



¹³C NMR of R3 (100 MHz, CDCl₃)



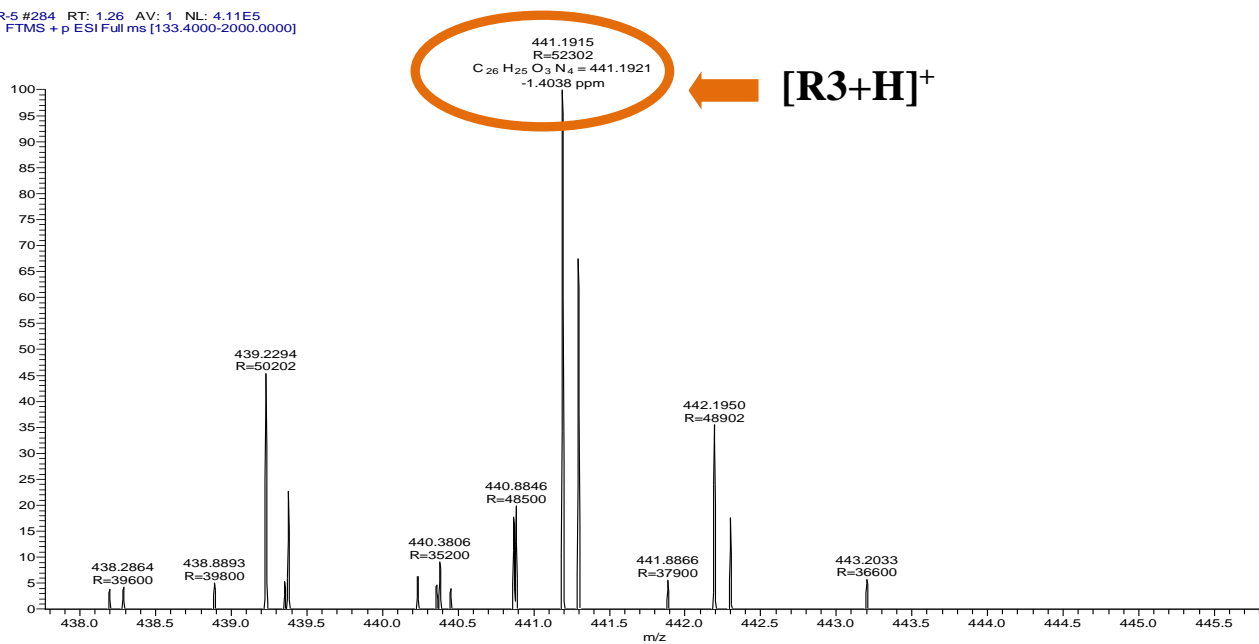
FT-IR spectra of R3:



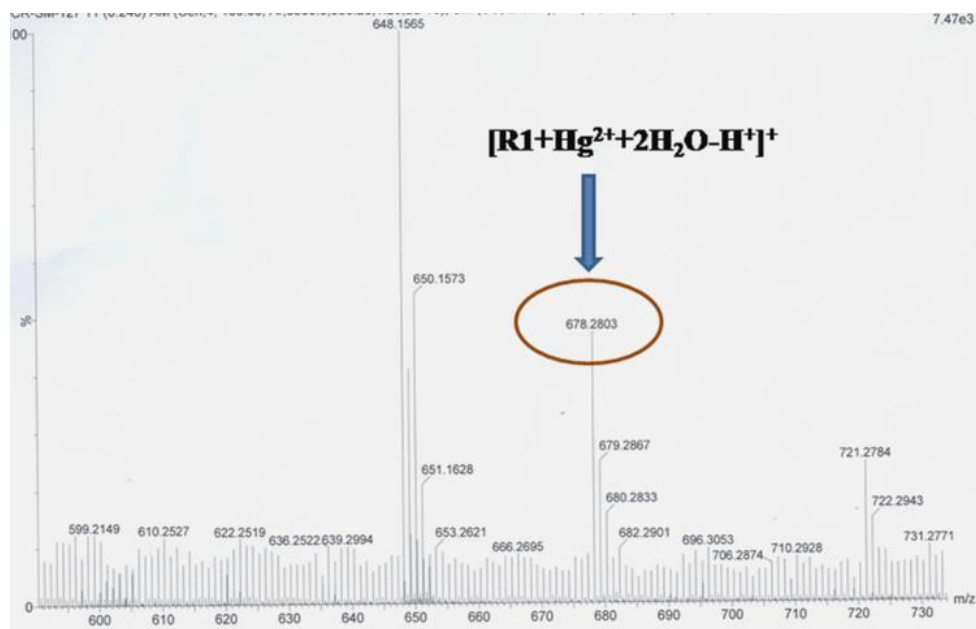
HRMS Spectra (R3):

Calculated: 440.1848, Mass: 441.1915 [M+H]⁺

JR-5 #284 RT: 1.26 AV: 1 NL: 4.11E5
T: FTMS + p ESI Full ms [133.4000-2000.0000]



Mass spectra of R1+Hg²⁺



FT-IR spectra of R1+Hg²⁺ complex:

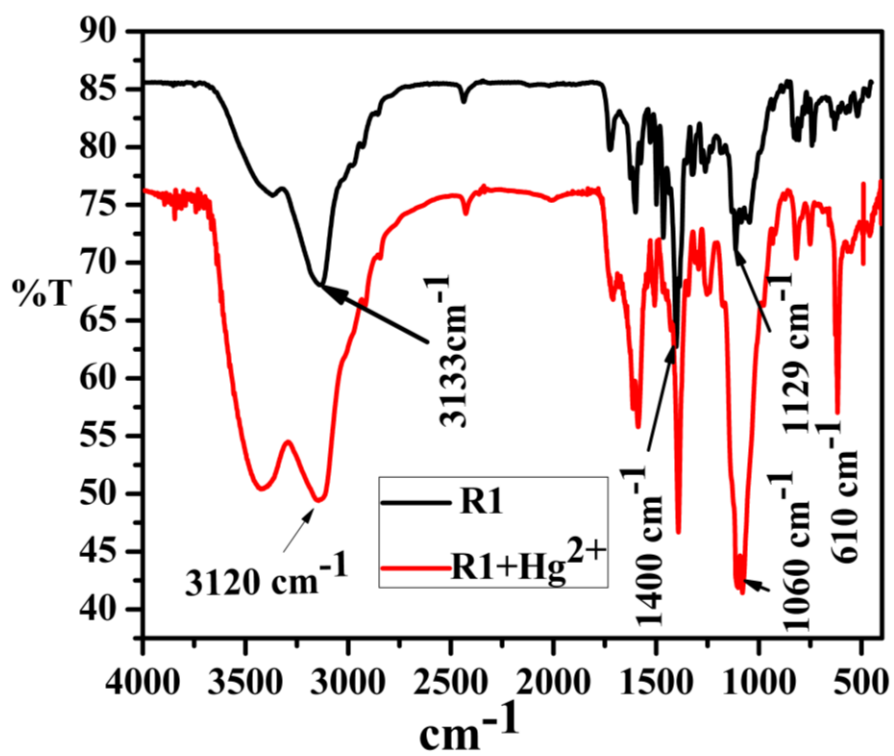


Table T1 Fluorescence decay parameters of coumarin amine (C)-quinoline (Q) mixtures and **R1** at $\lambda_{em}= 485$ nm (for coumarin) and 420 nm (for 8-OH quinoline).

Sample (λ_{em})	τ_1 (ns)	a_1	τ_2 (ns)	a_2	$\langle\tau\rangle$ (ns)
C	2.88				
Q	0.29	0.6149	1.075	0.3851	0.5059
Q:C::2:1 (420)	0.704	0.8836	2.51	0.116	0.913
Q:C::2:1 (485)	2.79				
Q:C::1:1 (420)	0.851	0.916	3.17	0.083	0.8053
Q:C::1:1 (485)	2.81				
Q:C::1:2 (420)	0.634	0.7265	1.87	0.2734	0.9718
Q:C::1:2 (485)	2.88				
R1(420)	0.795	0.735	2.54	0.264	1.254
R1(485)	2.428				

Table T2 Excited state decay parameters of **R1** with Hg^{2+} ; $\lambda_{em} = 485$ nm.

Sample (λ_{em})	τ_1 (ns)	a_1	τ_2 (ns)	a_2	$\langle\tau\rangle$ (ns)
R1	2.43				
R1Hg ²⁺ 6	0.623	0.469	2.51	0.530	1.622
R1 Hg ²⁺ 5	0.628	0.614	2.43	0.385	1.320
R1 Hg ²⁺ 4	0.77	0.850	3.04	0.149	1.11
R1 Hg ²⁺ 3	0.779	0.864	3.22	0.135	1.108
R1 Hg ²⁺ 2	0.817	0.891	3.37	0.108	1.092
R1 Hg ²⁺ 1	0.791	0.920	3.38	0.079	0.987

Table T3 Binding energy from DFT calculation.

Binding Mode	R1-Hg²⁺ energy (a. u.)	R1 Energy (a. u.)	Hg²⁺ energy (a. u.)	Binding Energy (a. u.)
A-mode	-1508.6479788128	-1466.4057308241	-41.7070505095	-0.5351974792
B-mode	-1508.6147256528	-1466.4057308241	-41.7070505095	-0.5019443192

Fig. S1 Absorption (a),(c) and emission spectra (b), (d) of **R2** and **R3** respectively with varying concentration of Hg^{2+} .

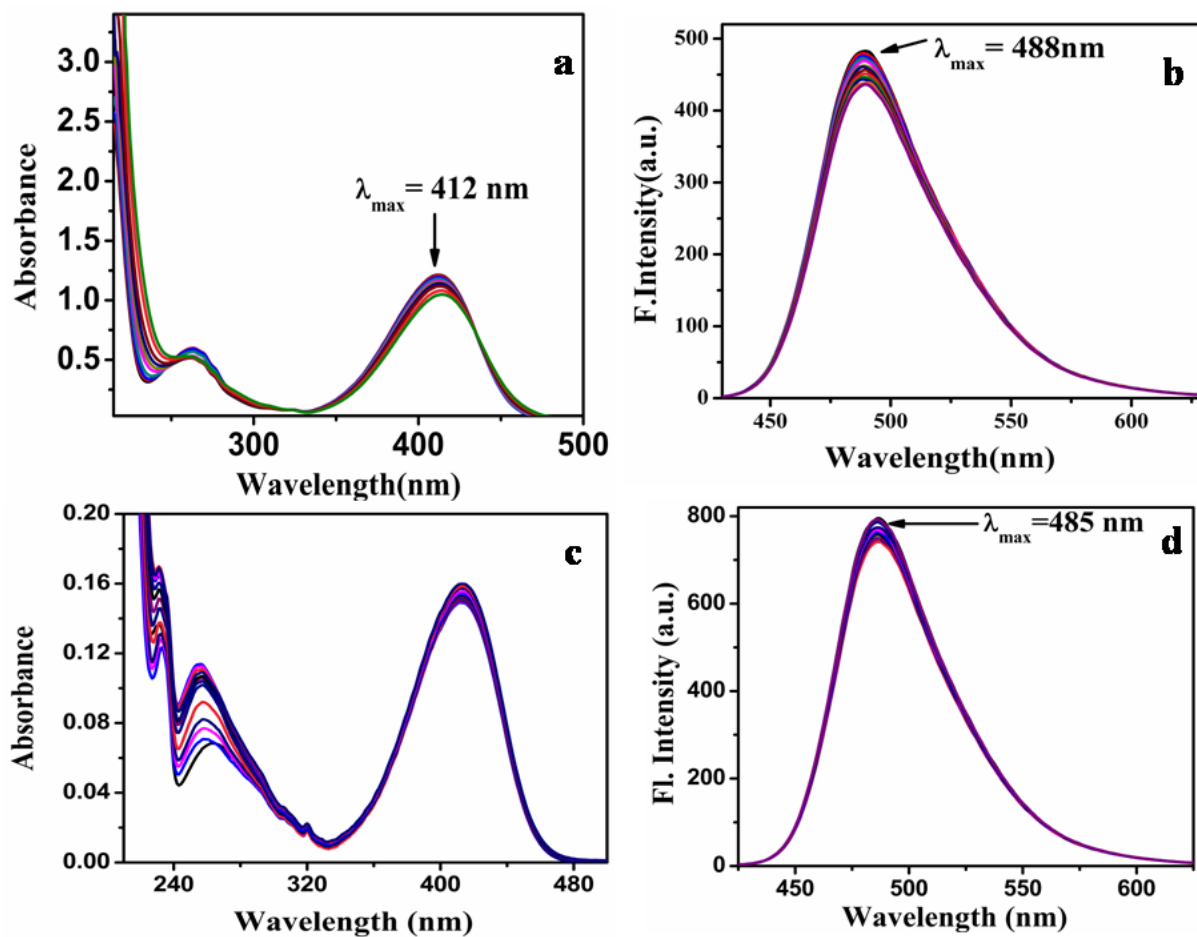


Fig. S2 Sensing behavior of **R1** towards Hg^{2+} under long UV.

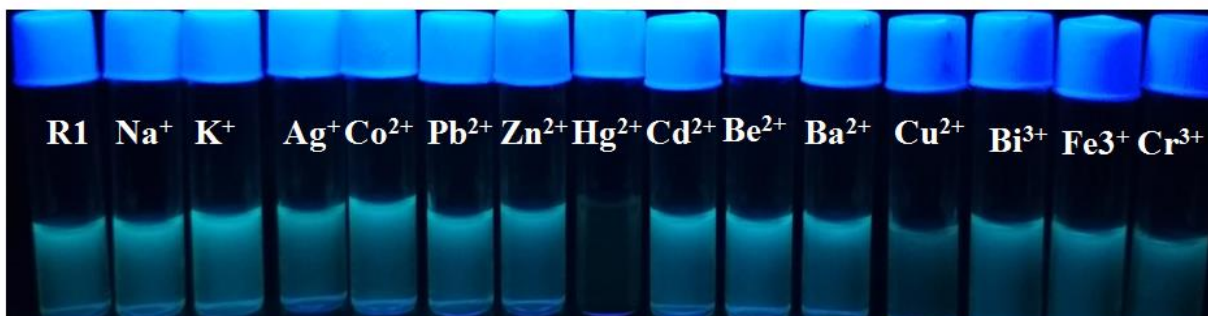


Fig. S3 S–V plots from steady state fluorescence emission intensity (inset shows deviation from linearity at higher concentration).

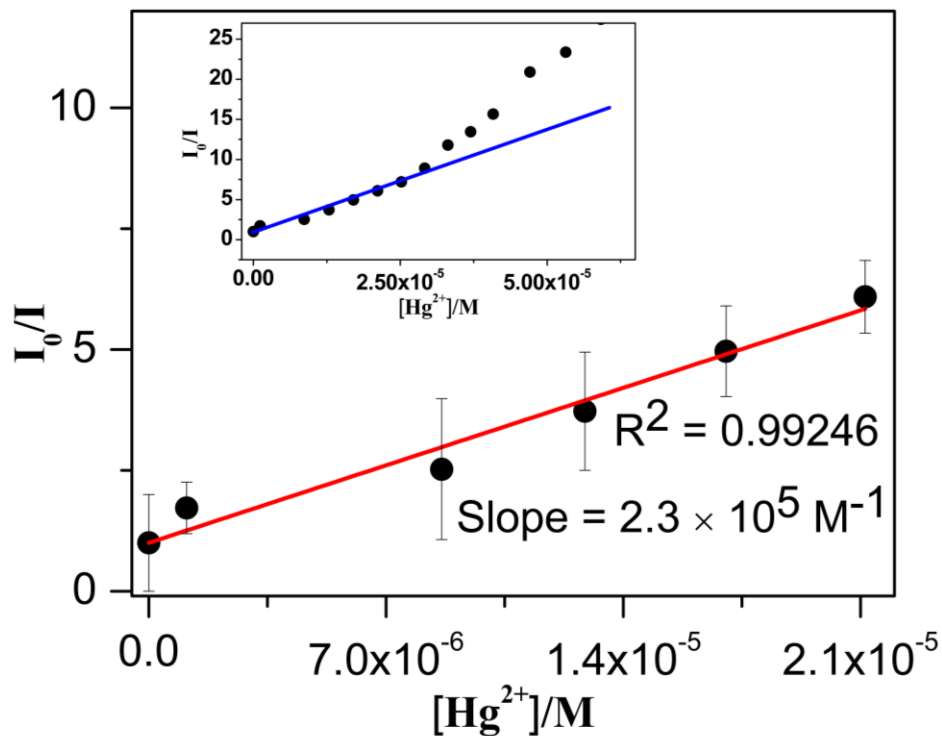


Fig. S4 Lifetime measurement with other metal ion.

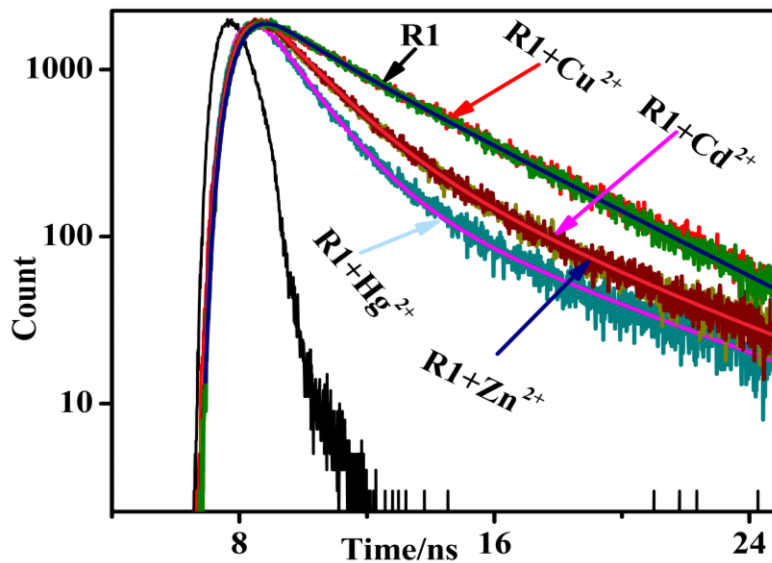


Fig. S5 Fluorescence decay traces of **R1** and quinoline-coumarin mixture (2:1) at $\lambda_{em}=485$ nm and 420 nm.

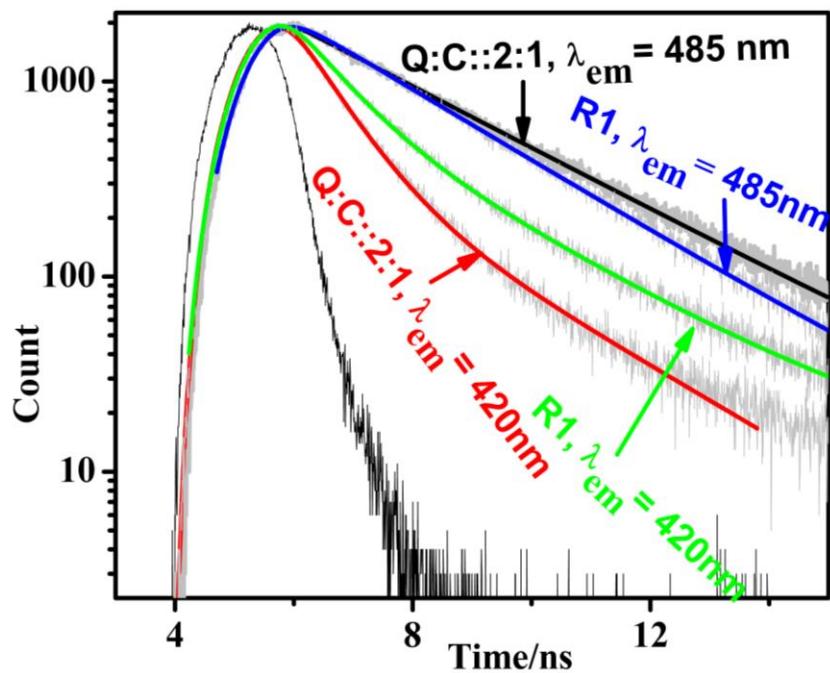
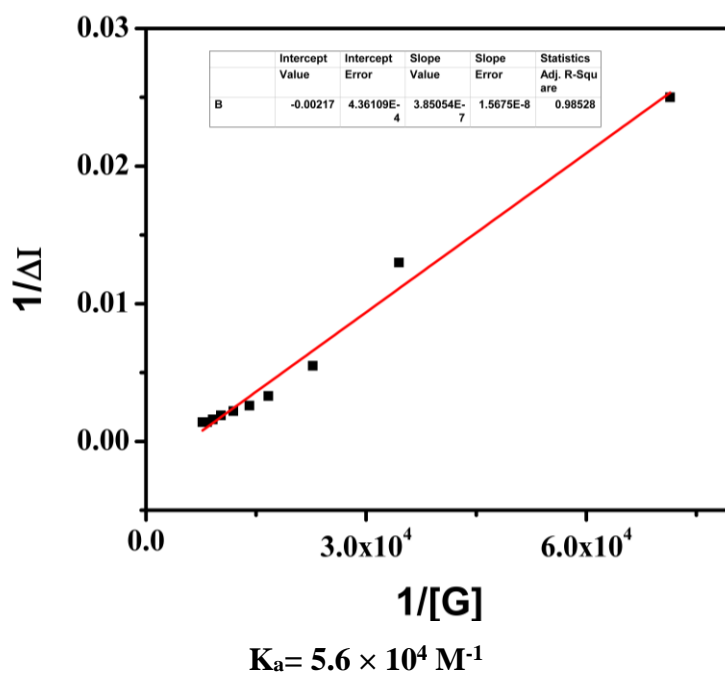


Fig. S6 Binding constant calculation graph of **R1** with Hg^{2+} using Fluorescence titration by using linear regression analysis.



Binding constant was calculated using Benesi-Hildebrand linear regression analysis following equation (i) where association constant $K_a = \text{intercept/slope}$. For this, the reciprocal of intensity difference ($1/\Delta I$), where $\Delta I = (I - I_0)$, was plotted against the reciprocal of concentration of guest ($1/[G]$)

$$1/(I - I_0) = 1/(I_\infty - I_0)K_a[G] + 1/(I_\infty - I_0) \quad \text{..... eqn. (i)}$$

Calculation of limit of detection (LOD):

Fluorescence titration data was used to calculate the limit of detection of **R1** with Hg^{2+} . To determine the standard deviation for the fluorescence intensity, the emission intensity of the individual receptors without any anion was measured by 10 times and the standard deviation of blank measurements was calculated. The limit of detection (LOD) of the receptor for sensing Hg^{2+} was determined from the following equation:

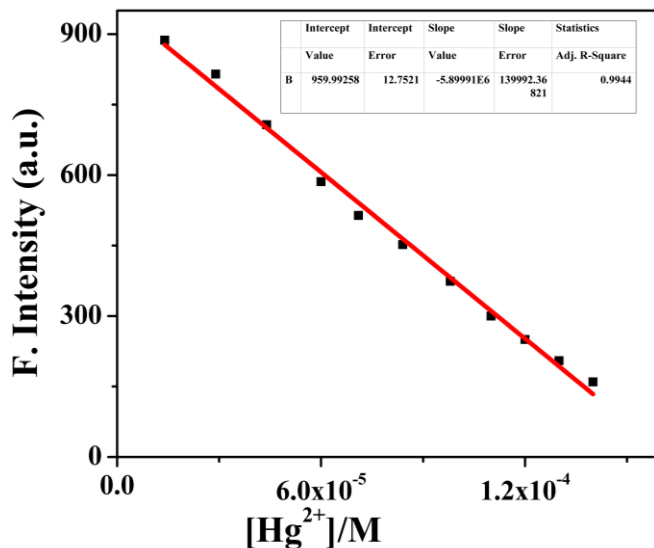
$$\text{LOD} = K \times \text{SD}/S$$

Where $K = 2$ or 3 (we take 3 in this case); SD is the standard deviation of the blank receptor (**R1**) solution; S is the slope of the calibration curve.

For R1 with Hg^{2+} :

From the linear fit graph, we get slope = 5.8×10^6 , and SD value is 0.51 . Thus using the above formula, we get the Limit of Detection = 1.728×10^{-7} M i.e. **R1** can detect Hg^{2+} up to this very lower concentration by fluorescence techniques.

Fig. S7 LOD calculation curve of **R1** with Hg^{2+} .



Reversibility Study:

Fig. S8 Reversibility test of receptor and R1+Hg^{2+} complex with EDTA.

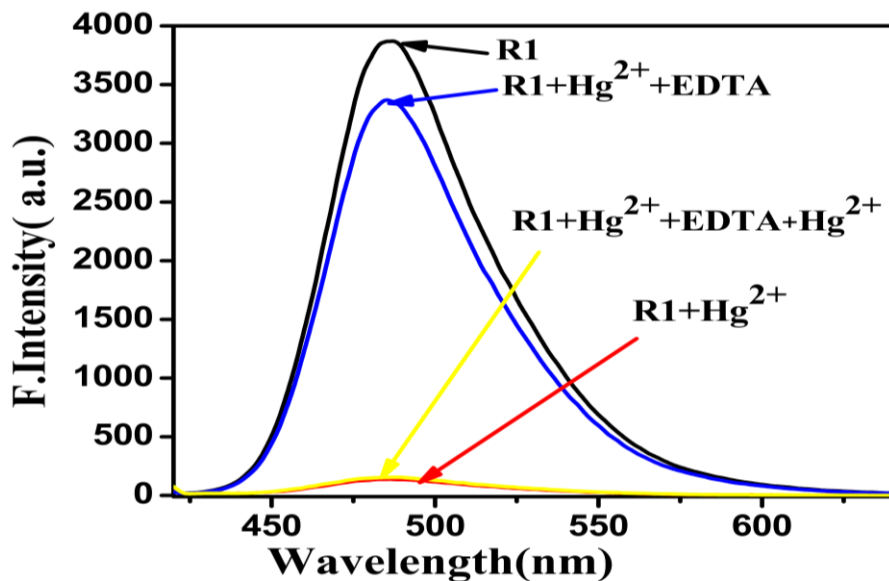
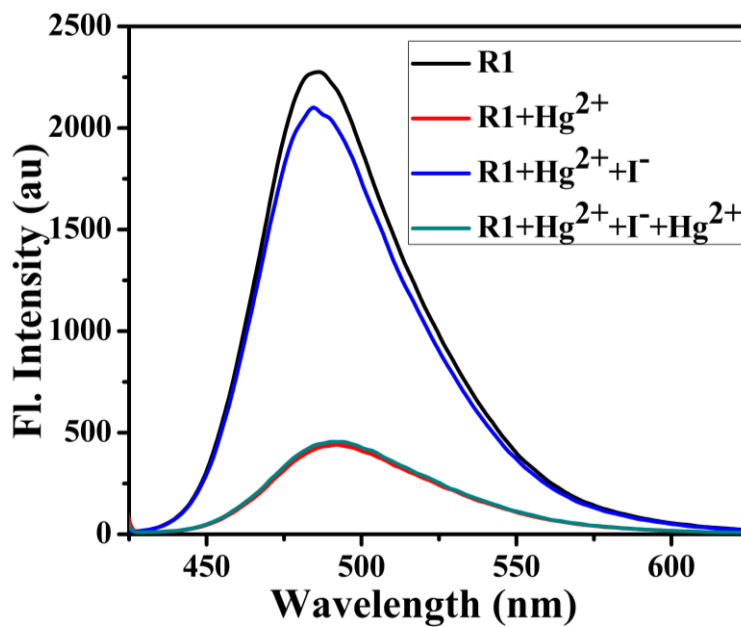


Fig. S9 Reversibility test of receptor and R1+Hg^{2+} complex with I^- .



Job's plot:

Fig. S10 Job's plot of R1 with Hg^{2+} indicating the formation of 1: 1 complex species.

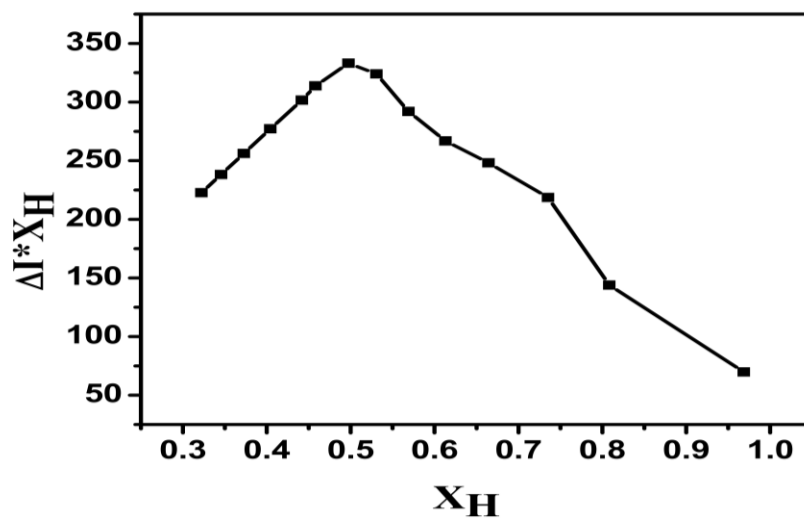


Fig. S11 Titration curve

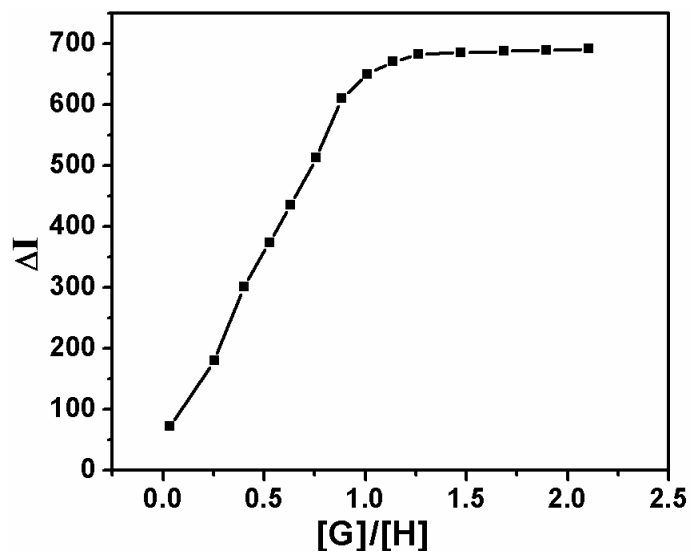


Fig. S12 Energy diagram for d-PET mechanism.

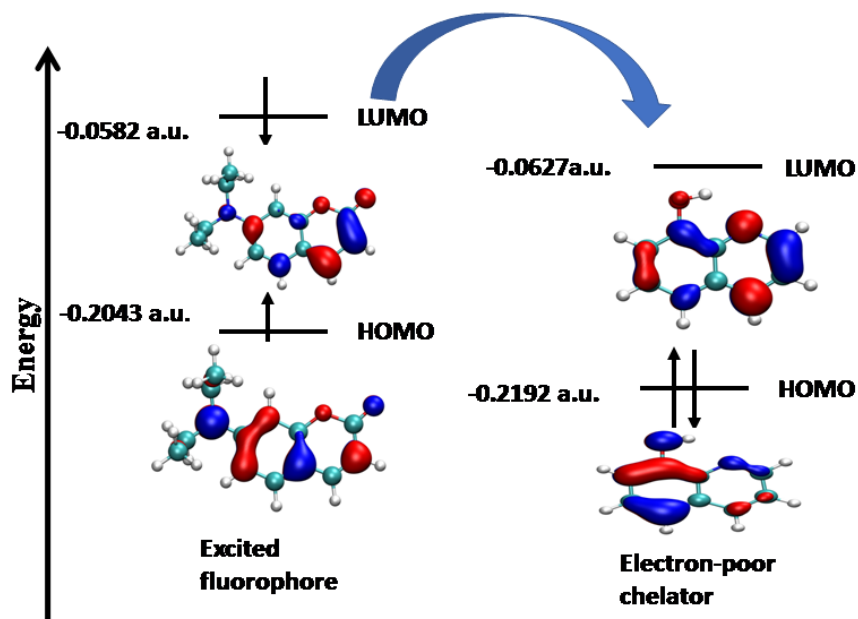
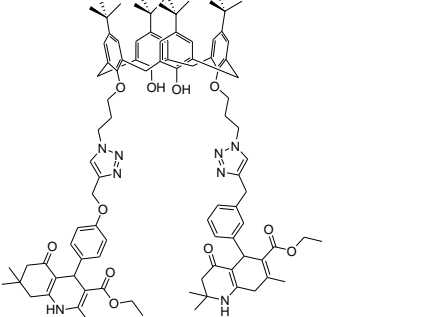
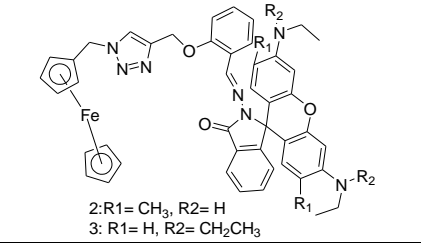
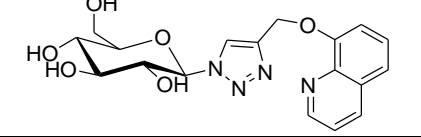
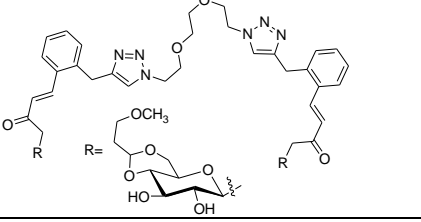
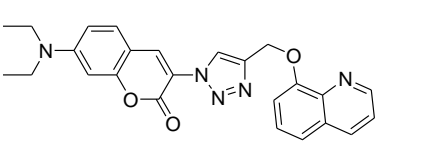


Table T4 Comparative table of triazole based sensor for Hg²⁺ from reported literature

Structures	Solvent	Selectivity/ Detection limit	Stoichiometry/ Crystal structure of receptors	Cell- Imaging study	Ref
	CH ₃ CN/H ₂ O(9 :1)	0.01 μM 0.44 μM	1:2/Not given	Not performed	1
	THF/H ₂ O(1:9)	Not Mentioned	Not Mentioned/ Not Given	Not performed	2
	CH ₃ CN/H ₂ O(5 :1)	0.09 μM(Hg ²⁺) 1.02 μM(Cu ²⁺)	1:2/ Not given	Not performed	3

	CH ₃ CN	2.0 μM	1:2/ Not Given	Performed	4
 2: R ₁ = CH ₃ , R ₂ = H 3: R ₁ = H, R ₂ = CH ₂ CH ₃	CH ₃ CN	3 ppb	1:1/ Not Given	Performed	5
	HEPES Buffer	Zn ²⁺ , Cd ²⁺ , Hg ²⁺	1:2, 1:2, 1:1 Respectively/ Given	Not performed	6
	CH ₃ CN	Ni ²⁺ , Hg ²⁺	1:1/ Not given	Not performed	7
	CH ₃ OH	Hg ²⁺ 17.2 μM	1:1/ All the three receptors are given	Performed	Present work

2. Experimental

*Preparation of 7-(Diethylamino)-3-nitro-2H-chromen-2-one(1) :*⁸

A mixture containing n-butanol (20 mL), 4-diethylamino salicylaldehyde (1.4 g, 7.2 mmol), ethyl nitroacetate (0.8 mL, 7.2 mmol), molecular sieves 4 Å (100 mg), piperidine (0.1 mL) and acetic acid (0.2 mL) was refluxed for a period of 24 h. Upon cooling to room temperature, a bright yellow solid formed, which was collected and dissolved in DMF (15 mL) at 80 °C. It was filtered again to remove the molecular sieves. The filtrate, upon addition to 100 ml of ice-cold water, yielded 3-nitro-7-diethylamino coumarin as a bright yellow solid: 1.40 g, 73 %. A small amount of this compound was recrystallized from DMF to give an analytical sample; m.p. 193-195 °C.

Preparation of 3-amino-7-(Diethylamino)-2H-chromen-2-one(2) :

In a 25 mL round bottomed flask equipped with a magnetic stirrer, were placed in order, 37.4% HCl (5 mL), stannous chloride dihydrate (1.6 g, 7.12 mmol). To this suspension 3-nitro-7-diethylamino coumarin (0.25 g, 0.95 mmol) was added at room temperature in small portions, over a period of thirty minutes. Stirring was continued for 4 h before the solution was poured onto 20 g of ice and made alkaline using sodium hydroxide solution (5 M) at 15 °C using an ice-water bath. The resulting suspension was then extracted with diethyl ether (2 X 25 mL). The organic layer was washed with water (50 mL), dried over anhydrous sodium sulfate and concentrated to a pasty residue which upon triturating using hexane yielded 3-amino-7-diethylaminocoumarin as a pale yellow solid: 0.15 g, 68%. A small amount of this compound was recrystallized in ethyl acetate / hexane to give an analytical sample; m.p. 85-87 °C.

Preparation of 3-azido-7-(Diethylamino)-2H-chromen-2-one(2) :

7-Diethylamino-3-amino coumarin (100 mg, 0.43 mmol) was dissolved slowly in HCl aq. (17.2%, 4 mL) at room temperature. Upon cooling to 0-5 °C and addition of a solution of NaNO₂ (30 mg, 0.43 mmol), the reaction mixture was stirred for 1 hour at 0-5 °C. This was followed by the addition of potassium acetate (2 g) in water (5 mL) to adjust the pH of the resulting solution to 4. Sodium azide (57 mg, 0.88 mmol) was added in portions at 0-5 °C, the mixture stirred at 0-5 °C for another five hours. The precipitated product was rapidly filtered, washed with ice-cold water (10 mL) and dried under vacuum to yield the final product as a yellow solid.

References

1. Shi, W. J.; Liu, J. Y.; Lo, P. C.; Ng, D. K., Selective Detection of Hg²⁺ Ions with Boron Dipyrromethene-Based Fluorescent Probes Appended with a Bis (1, 2, 3-Triazole) Amino Receptor. *Chem.: Asian J.* **2019**, *14*, 1059-1065.
2. Wei, G.; Jiang, Y.; Wang, F., A New Click Reaction Generated Aie-Active Polymer Sensor for Hg²⁺ Detection in Aqueous Solution. *Tetrahedron Lett.* **2018**, *59*, 1476-1479.
3. Huang, Y.; Li, C.-F.; Shi, W.-J.; Tan, H.-Y.; He, Z.-Z.; Zheng, L.; Liu, F.; Yan, J.-W., A near-Infrared Bodipy-Based Fluorescent Probe for Ratiometric and Discriminative Detection of Hg²⁺ and Cu²⁺ Ions in Living Cells. *Talanta* **2019**, *198*, 390-397.

4. Khan, B.; Hameed, A.; Minhaz, A.; Shah, M. R., Synthesis and Characterisation of Calix [4] Arene Based Bis (Triazole)-Bis (Hexahydroquinoline): Probing Highly Selective Fluorescence Quenching Towards Mercury (Hg²⁺) Analyte. *Journal of hazardous materials* **2018**, *347*, 349-358.
5. Arivazhagan, C.; Borthakur, R.; Ghosh, S., Ferrocene and Triazole-Appended Rhodamine Based Multisignaling Sensors for Hg²⁺ and Their Application in Live Cell Imaging. *Organometallics* **2015**, *34*, 1147-1155.
6. Areti, S.; Bandaru, S.; Rao, C. P., Triazole-Linked Quinoline Conjugate of Glucopyranose: Selectivity Comparison among Zn²⁺, Cd²⁺, and Hg²⁺ Based on Spectroscopy, Thermodynamics, and Microscopy, and Reversible Sensing of Zn²⁺ and the Structure of the Complex Using Dft. *ACS Omega* **2016**, *1*, 626-635.
7. Hemamalini, A.; Mudedla, S. K.; Subramanian, V.; Das, T. M., Design, Synthesis and Metal Sensing Studies of Ether-Linked Bis-Triazole Derivatives. *New J. Chem.* **2015**, *39*, 3777-3784.
8. Sivakumar, K.; Xie, F.; Cash, B. M.; Long, S.; Barnhill, H. N.; Wang, Q., A Fluorogenic 1, 3-Dipolar Cycloaddition Reaction of 3-Azidocoumarins and Acetylenes. *Org. Lett.* **2004**, *6*, 4603-4606.